On the Use of W-Band for Deep-Space Communications

S. Shambayati[1]

In this article, the performance of W-band (90 GHz) over a Deep Space Network's 34-m beam-waveguide (BWG) antenna is analyzed in terms of its average data return. In order to do so, data were collected from various sources about the performance of various W-band components. In addition, equations for calculating the W-band atmospheric noise temperature from water vapor radiometer 31.4-GHz sky-brightness measurements were obtained. Using these data it is shown that, even if the W-band link is operated optimally, due to weather effects the efficiency of the 34-m BWG antenna needs to be significantly improved from its current 18 percent efficiency to greater than 50 percent efficiency in order for the W-band link to return on the average significantly more (>2 dB) data than an optimum Ka-band link.

I. Introduction

With the push towards lower-weight and higher-speed spacecraft, the Deep Space Network is looking into using higher radio frequencies. This has a distinct advantage over the use of optical communications in that it uses existing DSN ground tracking facilities with some evolutionary modifications. Currently, the DSN is in the process of implementing Ka-band (32-GHz) tracking capabilities at all its tracking facilities. The next logical step is to look beyond Ka-band to W-band (90 GHz) to see whether or not W-band offers any significant advantage over Ka-band. This article reports on this inquiry.

The article is organized as follows: In Section II, the link equation for the average data rate is introduced and its optimization is discussed. This lays the foundation for the comparison of W-band's performance with that of Ka-band. As there are currently no W-band spacecraft or ground station components in existence for deep-space use, most of the analysis has been based on the experience and understanding of experts in various fields relating to deep-space communications. In Section III, the sources for the parameters used in this article as well as the formula for converting Ka-band water-vapor radiometer sky-brightness measurements to W-band zenith atmospheric noise-temperature measurements are given. In Section IV, equations in Sections II and III are used to calculate the value of "weather percentile" for the optimum performances for Ka-band, X-band, and W-band. (The term "weather percentile" is used as a shorthand to refer to the zenith atmospheric noise temperature associated with a fixed value of the cumulative distribution function (CDF). For example, if $\Pr\{T_z < T_0\} = 0.1$, then T_0 is said to be "10 percent weather.") In Section V, the performance of W-band is compared with those of Ka-band and X-band

[1] Communications Systems and Research Section.

The research described in this publication was carried out by the Jet Propulsion Laboratory, California Institute of Technology, under a contract with the National Aeronautics and Space Administration.

in the form of thermometer charts. In Section VI, performance of an optimum W-band link is compared with that of an optimum Ka-band link, and the required W-band break-even efficiencies (as compared to Ka-band) as a function of elevation for the W-band for the 34-m beam-waveguide (BWG) antenna are calculated. In addition, in Section VI the performance of an optimum W-band with an optimum Ka-band link is compared at different elevations for W-band ground antenna efficiencies of 18 percent (current 34-m BWG W-band efficiency). Furthermore, in Section VI the required W-band ground antenna efficiencies for a 2-dB W-band performance advantage over Ka-band were calculated. These results indicate that for elevations below 70 deg the ground antenna efficiency needs to be improved to better than 50 percent (>70 percent at 30 deg) in order for the W-band to offer 2-dB better performance than Ka-band. In Section VII, a conclusion and caveats are discussed.

The results in this article indicate that W-band is severely hampered by weather effects. In addition, since the DSN 34-m BWG antennas [1] are designed for frequencies lower than W-band, the efficiency of these antennas needs to be greatly improved before W-band could compete with Ka-band. Furthermore, projected (as there are none planned to be designed or built) W-band spacecraft amplifiers are rather inefficient. Compared to these factors, losses due to spacecraft antenna efficiency and ground and spacecraft pointing losses are relatively minor. The analysis here focuses mostly on the interaction between ground antenna efficiency and the weather. Specifically, the analysis considers the necessary efficiency of the ground antenna at W-band at a particular weather percentile if the W-band link is to have the same performance as Ka-band at a given (but necessarily the same as W-band) weather percentile for different elevations.

II. Link Equation for Average Data Rate

The power performance of a link could be analyzed using the standard link equation. The link equation describes the received signal-to-noise ratio on the ground, P_r/N_0, as

$$\frac{P_r}{N_0} = P_{Amp} \times \varepsilon_{Amp} \times \frac{4\pi^2 \times r_{sc}^2}{\lambda^2} \times \varepsilon_{sc} \times L_{psc}^{-1} \times \left(\frac{\lambda}{d}\right)^2 \times L_{Atm}^{-1}$$

$$\times L_{pg}^{-1} \times \frac{4\pi^2 \times r_G^2}{\lambda^2} \times \varepsilon_G \times (k \times T_{sys})^{-1} \tag{1}$$

In this equation, P_{Amp} is the power into the spacecraft amplifier; ε_{Amp} is the amplifier efficiency; λ is the RF wavelength; r_{sc} and r_G are spacecraft and ground antenna radii, respectively; L_{psc} and L_{pg} are the spacecraft and ground pointing losses, respectively; ε_{sc} and ε_G are the spacecraft and ground antenna efficiencies, respectively; and d is the distance between the spacecraft and the Earth. L_{Atm} is the loss due to atmospheric absorption; T_{sys} is the ground system noise temperature; and k is Boltzman's constant.

When a link is designed, certain assumptions are made about the parameters in Eq. (1) that are related both to the spacecraft and the ground system's physical characteristics and the link design philosophy. The most important assumption in the link design is made about the value of T_{atm}, the atmospheric noise temperature. Atmospheric noise temperature affects two parameters in Eq. (1): atmospheric loss, L_{Atm}, and the system noise temperature, T_{sys}. The atmospheric loss, L_{Atm}, is related to T_{atm} through the following approximation [2]:

$$L_{Atm} \approx \begin{cases} \dfrac{275}{275 - T_{atm}}, & T_{atm} < 275 \\ \infty, & \text{otherwise} \end{cases} \tag{2}$$

Note that, since the absorption loss of the atmosphere depends on the length of the path that the signal takes through the atmosphere, the atmospheric loss at any given elevation, θ_0, can be converted to the atmospheric loss at any other elevation, θ, by

$$L_{Atm}(\theta) = \left[L_{Atm}(\theta_0)\right]^{(\sin\theta_0)/(\sin\theta)} \tag{3}$$

Note that Eq. (3) assumes a flat Earth model. Setting $\theta_0 = 90$ deg and atmospheric noise temperature at an elevation θ, $T_{atm}(\theta)$ is obtained from the zenith atmospheric noise temperature, $T_Z = T_{atm}(90\text{ deg})$, using Eqs. (2) and (3) by

$$T_{atm}(\theta) = \left(1 - L_Z^{-(1/\sin\theta)}\right) 275 \tag{4}$$

where L_Z, the zenith atmospheric loss, is given by

$$L_Z = \begin{cases} \dfrac{275}{275 - T_Z}, & T_Z < 275 \\ \infty, & \text{otherwise} \end{cases} \tag{5}$$

The system noise temperature, T_{sys}, is a figure of merit that reflects how noisy the system is. It consists of equipment noise temperature, atmospheric noise temperature, and observed cosmic background noise. At elevation θ, T_{sys} is given by

$$T_{sys}(\theta) = T_{eq}(\theta) + T_{atm}(\theta) + \frac{2.7}{L_{Atm}(\theta)} \tag{6}$$

$T_{eq}(\theta)$ is the equivalent noise temperature of the ground equipment and is a deterministic function of the elevation. Cosmic background noise contribution to the overall system noise is represented by $2.7/L_{atm}(\theta)$. Using Eq. (4), Eq. (6) can be modified to

$$T_{sys}(\theta) = 275 - 272.3 L_Z^{-(1/\sin\theta)} + T_{eq}(\theta) \tag{7}$$

Defining the sky-brightness temperature at elevation as

$$T_B(\theta) = 275 - 272.3 L_Z^{-(1/\sin\theta)} \tag{8}$$

Eq. (7) can be written as

$$T_{sys}(\theta) = T_{eq}(\theta) + T_B(\theta) \tag{9}$$

The importance of sky-brightness temperature becomes clear when formulas for converting Ka-band sky-brightness temperature measurements to W-band sky-brightness temperature measurements are introduced.

Since the weather is time varying, so is the atmospheric contribution to the system performance as described in Eq. (1). This means that a certain fraction of the time the link will not be available because the design zenith atmospheric noise temperature, $T_Z^{(d)}$, is lower than the actual zenith atmospheric noise temperature. Therefore, the average data rate at elevation θ, $R(\theta)$, is proportional to the product of the designed received power-to-noise ratio, $P_r/N_0\left(\theta, T_Z^{(d)}\right)$, and the probability that the actual zenith atmospheric noise temperature is less than $T_Z^{(d)}$. In other words,

$$R(\theta) \propto \Pr\left\{T_Z \le T_Z^{(d)}\right\} \times \frac{P_r}{N_0}\left(\theta, T_Z^{(d)}\right) \tag{10}$$

Equation (10) is the link equation for average data rate at elevation θ. Note that, at any elevation θ, Eq. (10) can be maximized with respect to $T_Z^{(d)}$. Thus, the performance of the link could be optimized at any elevation.

Now let $R_{opt}^{(W)}\left(\theta, \varepsilon_G^{(W)}\right)$ be the optimum data rate for W-band at elevation θ when the ground antenna's W-band efficiency is $\varepsilon_G^{(W)}$ and let $R_{opt}^{(Ka)}\left(\theta, \varepsilon_G^{(Ka)}\right)$ be the optimum Ka-band data rate at elevation θ. Furthermore, let $T_{Z,opt}^{(W)}(\theta)$ be the optimum zenith atmospheric noise temperature for W-band at elevation θ; $T_{Z,opt}^{(Ka)}(\theta)$ be the optimum zenith atmospheric noise temperature for Ka-band at elevation θ; and define $p_{opt}^{(W)}(\theta) = \Pr\left\{T_Z \le T_{Z,opt}^{(W)}(\theta)\right\}$ and $p_{opt}^{(Ka)}(\theta) = \Pr\left\{T_Z \le T_{Z,opt}^{(Ka)}(\theta)\right\}$. In order for W-band to support the same average data rate at elevation θ as does Ka-band, equality $R_{opt}^{(W)}\left(\theta, \varepsilon_G^{(W)}\right) = R_{opt}^{(Ka)}\left(\theta, \varepsilon_G^{(Ka)}\right)$ needs to hold. Assuming that the spacecraft power, antenna size, and antenna efficiency are the same for both W-band and Ka-band and using Eqs. (1), (9), and (10), equality $R_{opt}^{(W)}\left(\theta, \varepsilon_G^{(W)}\right) = R_{opt}^{(Ka)}\left(\theta, \varepsilon_G^{(Ka)}\right)$ is reduced to

$$\begin{aligned}&\varepsilon_{Amp}^{(Ka)} \times \frac{1}{\lambda_{Ka}^2} \times \varepsilon_G^{(Ka)} \times \left(T_{eq}^{(Ka)}(\theta) + T_B^{(Ka)}(\theta)\right)^{-1} \times p_{opt}^{(Ka)}(\theta) \times \left(L_{psc}^{(Ka)} \times L_{Atm}^{(Ka)}(\theta) \times L_{pg}^{(Ka)}\right)^{-1} \\ &= \varepsilon_{Amp}^{(W)} \times \frac{1}{\lambda_W^2} \times \varepsilon_G^{(W)} \times \left(T_{eq}^{(W)}(\theta) + T_B^{(W)}(\theta)\right)^{-1} \times p_{opt}^{(W)}(\theta) \times \left(L_{psc}^{(W)} \times L_{Atm}^{(W)}(\theta) \times L_{pg}^{(W)}\right)^{-1}\end{aligned} \tag{11}$$

Using this equation, the W-band break-even efficiency (as compared to Ka-band) at elevation θ is defined as

$$\varepsilon_{W,Ka}(\theta) = \varepsilon_G^{(Ka)} \times \frac{\varepsilon_{Amp}^{(Ka)}}{\varepsilon_{Amp}^{(W)}} \times \frac{L_{psc}^{(W)}}{L_{psc}^{(Ka)}} \times \frac{L_{Atm}^{(W)}(\theta)}{L_{Atm}^{(Ka)}(\theta)} \times \frac{L_{pg}^{(W)}}{L_{pg}^{(Ka)}} \times \frac{\lambda_W^2}{\lambda_{Ka}^2} \times \frac{T_{sys}^{(W)}(\theta)}{T_{sys}^{(Ka)}(\theta)} \times \frac{p_{opt}^{(Ka)}(\theta)}{p_{opt}^{(W)}(\theta)} \tag{12}$$

Alternatively, the relative advantage (disadvantage) of W-band over Ka-band is given by

$$A_{W,Ka}(\theta) = \frac{\varepsilon_{AMP}^{(W)}}{\varepsilon_{AMP}^{(Ka)}} \times \frac{L_{psc}^{(Ka)}}{L_{psc}^{(W)}} \times \frac{L_{Atm}^{(Ka)}(\theta)}{L_{Atm}^{(W)}(\theta)} \times \frac{L_{pg}^{(Ka)}}{L_{pg}^{(W)}} \times \frac{\lambda_{Ka}^2}{\lambda_W^2} \times \frac{\varepsilon_G^{(W)}}{\varepsilon_G^{(Ka)}} \times \frac{T_{sys}^{(Ka)}(\theta)}{T_{sys}^{(W)}(\theta)} \times \frac{p_{opt}^{(W)}(\theta)}{p_{opt}^{(Ka)}(\theta)} \tag{13}$$

Converting Eq. (13) into decibels, the following is obtained:

$$\Delta_{W,Ka}(\theta) = \Delta_{\varepsilon_{AMP}} - \Delta_{L_{psc}} - \Delta_{L_{Atm}}(\theta) - \Delta_{L_{pg}} + \Delta_{\varepsilon_G} - \Delta_{T_{sys}}(\theta) + \Delta_{p_{opt}} + 8.98 \text{ dB} \tag{14}$$

Note that

$$8.98 \text{ dB} = 10 \times \log \left(\frac{\lambda_{Ka}^2}{\lambda_W^2} \right) = 20 \times \log \left(\frac{90 \text{ GHz}}{32 \text{ GHz}} \right)$$

Using Eqs. (11) through (14), the performance of the W-band link will be compared to that of Ka-band. In the next section, the sources for populating the parameters for these equations are discussed.

III. Sources of Parameters

In order to perform the analysis outlined in the previous section, some information is needed about the parameters used in the equations. Information for Ka-band is rather sparse as there have been only four spacecraft that have flown Ka-band (Mars Observer, Mars Global Surveyor, Deep Space 1 (DS1), and Cassini). Furthermore, currently Ka-band has been implemented on only one operational antenna (DSS 25). In addition, a statistically significant amount of data for atmospheric noise-temperature measurements for the Canberra Deep Space Communications Complex (CDSCC) is not available. Data exist for four spacecraft amplifiers, the latest being a 35-W traveling-wave tube amplifier (TWTA) with 48 percent efficiency. This is the amplifier that most likely is to be used on a future Ka-band mission and currently is slated to fly on Mars Reconnaissance Orbiter (MRO). Ground antenna efficiencies are available for Ka-band. The 34-m beam-waveguide antennas have an efficiency of 61.19 percent (see [1]) at the rigging angle. Due to the fact that these antennas are rather rigid, their efficiency does not change much with changes in the elevation. The ground equipment noise-temperature contribution to the total ground system noise contribution is approximately 32.3 K (again see [1]).

As sparse as the data for Ka-band are, compared to W-band they are a treasure trove. For W-band, *no* direct measurements of atmospheric noise temperature are available. However, Stephen Keihm has been able to create a model for converting 31.4-GHz sky-brightness temperature measurements to 90-GHz sky-brightness values based on radio sound measurements.[2] These equations are for the Goldstone and Madrid Deep Space Communication Complexes (GDSCC and MDSCC). After further consultation with Stephen Keihm, it was decided that the conversion formula for Madrid also applies to Canberra, even though no direct radio sound measurements exist for Canberra. The formula for converting 31.4-GHz zenith sky-brightness temperature, given by Eq. (8), to 90-GHz zenith sky-brightness temperature for Goldstone is given by

$$T_B^{(W)} = -19.77 + 4.3259\, T_B^{(Ka)} - 0.0186 \left(T_B^{(Ka)} \right)^2 \tag{15}$$

For Madrid and Canberra, this conversion formula is given by

$$T_B^{(W)} = -25.84 + 4.7810\, T_B^{(Ka)} - 0.0222 \left(T_B^{(Ka)} \right)^2 \tag{16}$$

Very few data are available for W-band spacecraft amplifiers. The best guess (and it is only an educated guess, by Anthony Mittskus, because there is no such amplifier in development) is that such an amplifier, depending on technology, is going to be at best 25 to 30 percent efficient (this is for a ~35-W tube; solid-state power amplifiers (SSPAs) are going to be less than 10 percent efficient).[3] Based on measurements

[2] S. Keihm, Jet Propulsion Laboratory, Section 386, Pasadena, California, 2002.

[3] A. Mittskus, Jet Propulsion Laboratory, Section 336, Pasadena, California, 2002.

performed at DSS 13, a 34-m BWG is only 18 percent efficient at W-band in its current configuration.[4] Based on measurements performed jointly by TRW and JPL, the noise contribution of a low-noise amplifier (LNA) to the system noise is between 40 K and 60 K.[5] The efficiency of spacecraft antennas is rather high. Based on the data obtained from the CLOUDSAT antenna, the antenna efficiency is at least 85 percent.[6] Other factors, such as circuit losses on the spacecraft, are ignored in this study as that is mostly a function of design. Based again on results obtained for CLOUDSAT, the circuit losses at W-band are about 0.1 dB per inch. All this information is tabulated in Table 1.

There are some common parameters that are translated into losses for the link. These are antenna-pointing accuracies both for the ground and the spacecraft (0.035 deg for the spacecraft, according to Bob Oberto and Bob Kinsey,[7] and 0.001 deg for the ground antenna for a 34-m BWG antenna, based on measurements with Ka-band monopulse made by Hamil Cooper.[8] This information is also included in Table 1.

Since in Section V the X-band performance is also compared to those of W-band and Ka-band, X-band performance parameters also were obtained. These parameters are highly reliable and are based on years of X-band operations. They include full knowledge of atmospheric noise-temperature statistics

Table 1. W-band parameters and their sources.

Parameter	Value	Source	Comments
Spacecraft antenna efficiency	85%	Suzanne Spitz	Based on measurements of the CLOUDSAT antenna.
W-band circuit losses	0.1 dB/in.	Suzanne Spitz	Based on measurements for CLOUDSAT.
W-band atmospheric noise temperature	Conversion formulas	Stephen Keihm	Radio sound measurements for Goldstone and Madrid. Madrid formula deemed usable for Canberra.
Spacecraft amplifier efficiency	25% to 30%	Anthony Mittskus	Best guess. Extremely favorable numbers. Constitutes an upper bound on the efficiency.
Ground antenna efficiency	18%	Larry Teitelbaum	Actual measurements at DSS 13.
Ground amplifier noise temperature	40 K to 60 K	Javier Batista	Work of Section 386 with TRW. Results obtained by Todd Gaier.
Spacecraft 3-sigma pointing	0.035 deg	Bob Oberto and Bob Kinsey	Actual attitude control systems currently available.
Ground antenna 3-sigma pointing	0.001 deg	Hamil Cooper	Based on Ka-band monopulse measurements at DSS 13. Could be different for W-band if a W-band-specific active pointing mechanism were used.

[4] Obtained from L. Teitelbaum, Jet Propulsion Laboratory, Section 333, Pasadena, California, 2002.

[5] J. Batista, personal communication, Jet Propulsion Laboratory, Section 333, Pasadena, California, 2002. Batista conveyed results obtained by T. Gaier, Jet Propulsion Laboratory, Section 386, Pasadena, California, 2002.

[6] Obtained from S. Spitz, Jet Propulsion Laboratory, Section 336, Pasadena, California, 2002.

[7] R. Oberto and R. Kinsey, Jet Propulsion Laboratory, Section 311, Pasadena, California, 2002.

[8] H. Cooper, Jet Propulsion Laboratory, Section 333, Pasadena, California, 1999.

at all three DSCC sites (see [2]), LNA noise contribution (∼22.2 K; see [1]), ground antenna efficiency (76.66 percent for a 34-m BWG antenna; see [1]), and spacecraft amplifier efficiency (∼60 percent for the 100-W X-band TWTA used on MRO).

Using Eqs. (15) and (16), the W-band curves shown in Figs. 1(a) through 1(c) and Table 2 are obtained. As seen from the figures, for the same value of weather percentile, the zenith atmospheric noise temperature for W-band is significantly larger than those for Ka-band and X-band. As will be shown in Sections V and VI, this significantly increases the system noise temperature for W-band and thus eliminates any advantage that the increase in frequency may provide the W-band.

IV. Optimum W-Band, Ka-Band, and X-Band Weather

In order to compare W-band fairly with X-band and Ka-band, it was decided to calculate the optimum weather for elevations between 10 deg and 90 deg for all three bands by maximizing Eq. (10) for a 34-m BWG antenna at the three DSCCs at Goldstone, Madrid, and Canberra. The results of this optimization are shown in Figs. 2 through 4. Each figure displays contours of constant average data rate expressed in decibels versus elevation and weather percentile. The approximate path of maximum ascent through these contours is identified in each figure. For a given elevation, the weather percentile identified by this path corresponds to the optimum weather percentile for that elevation. Figures 2(a) through 2(c) indicate that the optimum weather percentile for X-band is between 89 percent and 96 percent, depending on the site and elevation. Figures 3(a) through 3(c) indicate that Ka-band performs optimally at less weather reliability, with the optimum performance occurring between 72 percent and 92 percent, depending on the site and the elevation. As seen from Figs. 4(a) through 4(c), W-band has even lower weather reliability than does Ka-band for its optimal performance (between 53 percent and 87 percent, depending on the site and elevation).

Table 2. W-band atmospheric noise-temperature cumulative distribution.

Weather percentile	Goldstone	Madrid	Canberra
10	21.687141	22.89088	28.623277
20	24.452576	28.509615	32.954707
25	25.611155	30.697421	34.873506
30	26.759794	32.877172	36.756644
40	29.32458	37.258003	40.85665
50	32.509651	41.300124	45.33843
60	36.236936	45.51572	51.213216
70	40.896118	50.249545	59.31611
75	43.856766	52.916617	64.311271
80	47.232872	55.967577	70.842008
85	51.003046	60.620257	80.255377
90	55.74443	71.854662	94.363194
92.5	59.352375	87.796332	105.709304
95	66.038401	119.615953	125.184375
97.5	87.930701	173.240388	168.651488
99	123.867923	210.61154	212.965139

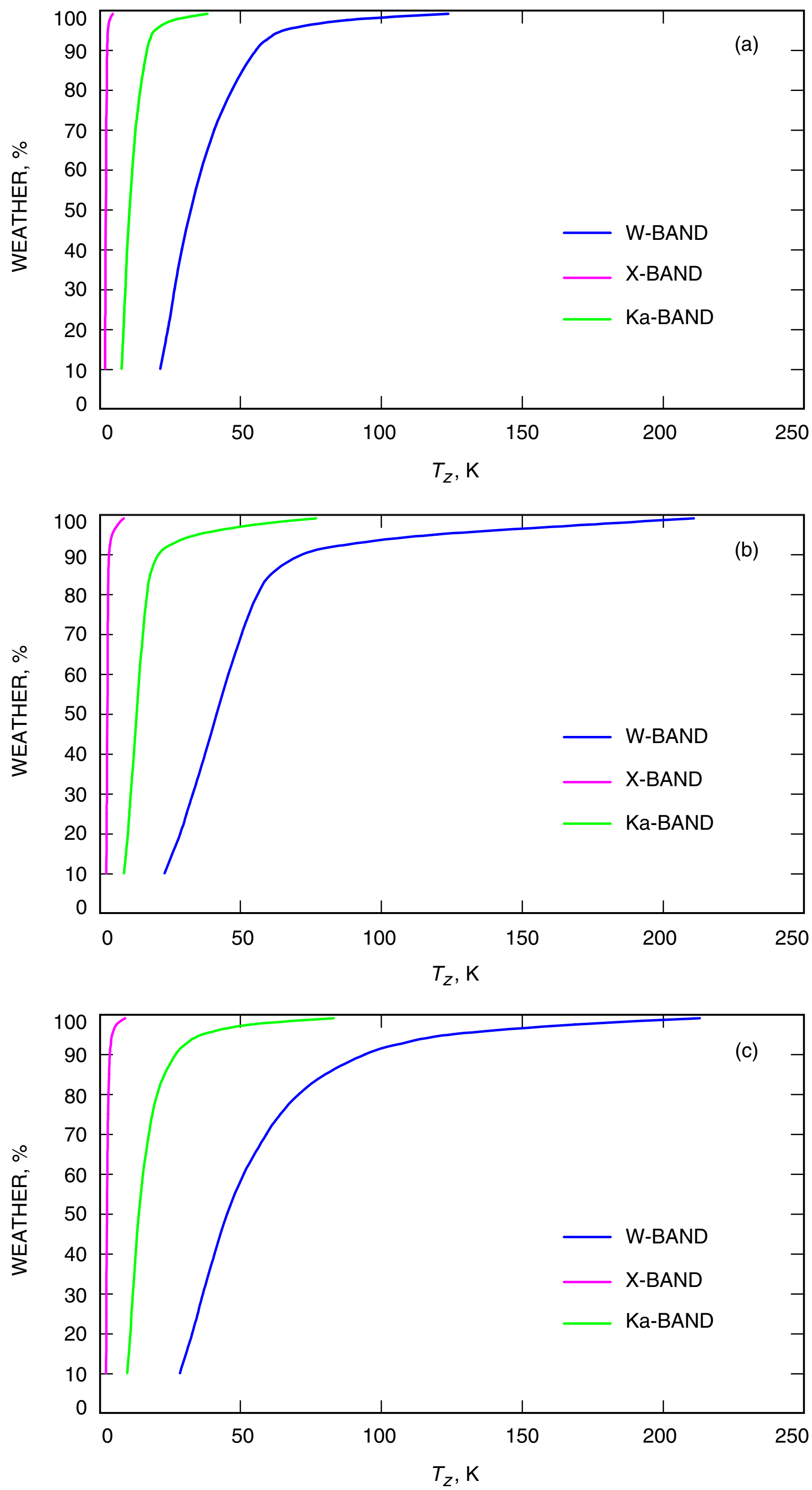

Fig. 1. Zenith atmospheric noise-temperature CDF versus zenith atmospheric noise temperature for W-band, X-band, and Ka-band: (a) Goldstone, (b) Madrid, and (c) Canberra.

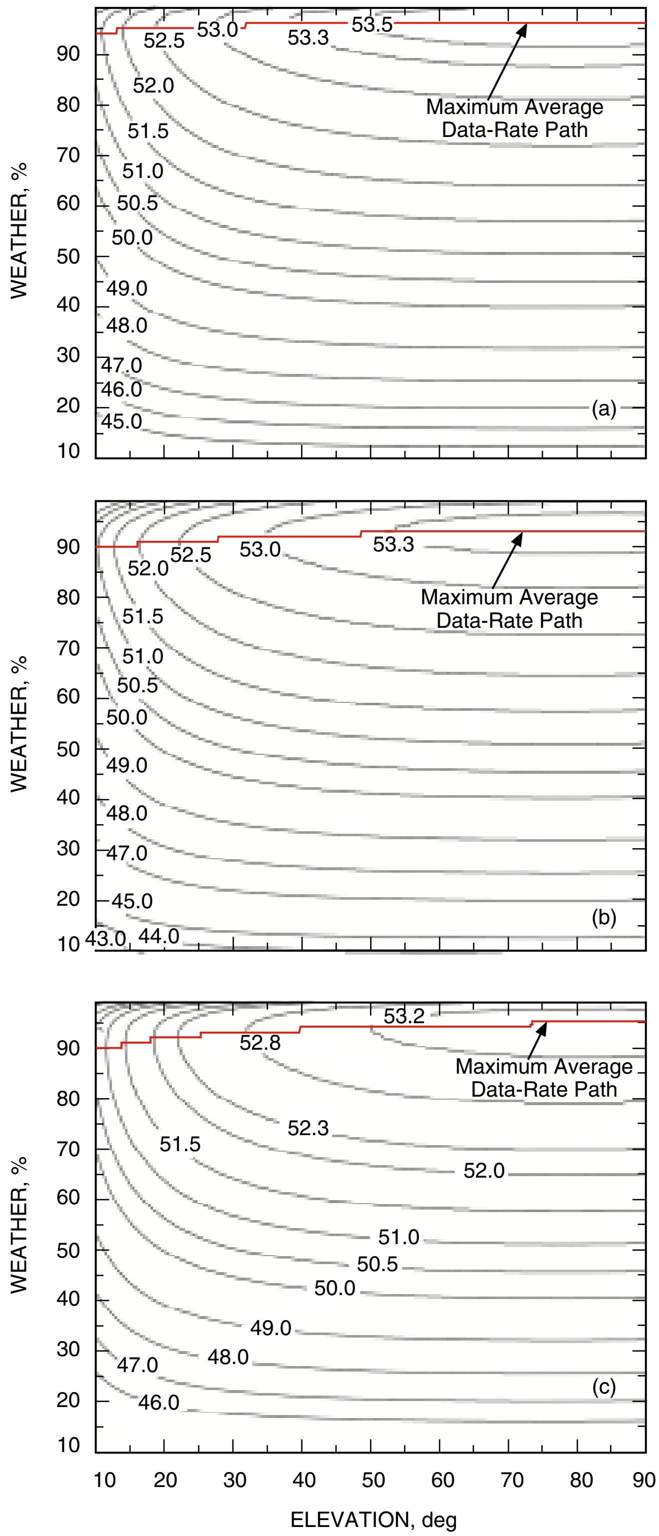

Fig. 2. Contours of average data rate versus elevation and weather percentile for X-band: (a) Goldstone, (b) Madrid, and (c) Canberra.

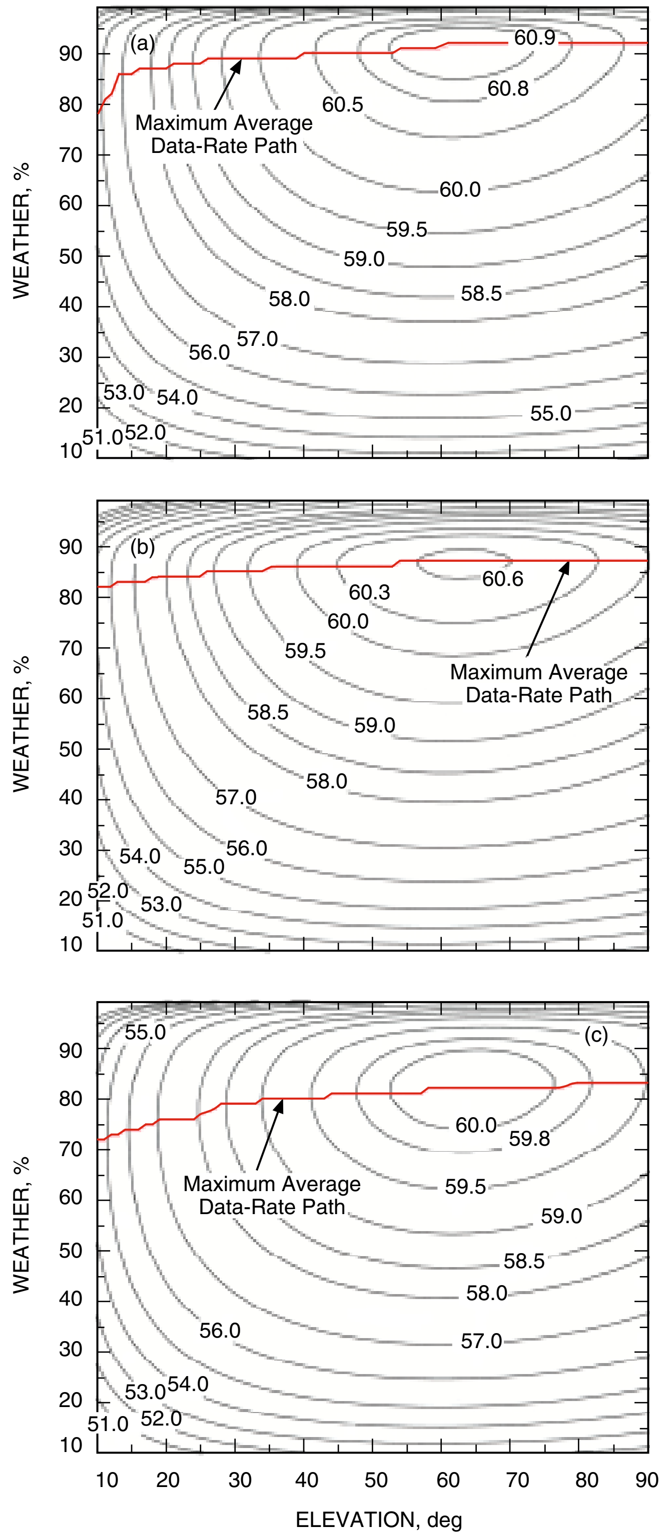

Fig. 3. Contours of average data rate versus elevation and weather percentile for Ka-band: (a) Goldstone, (b) Madrid, and (c) Canberra.

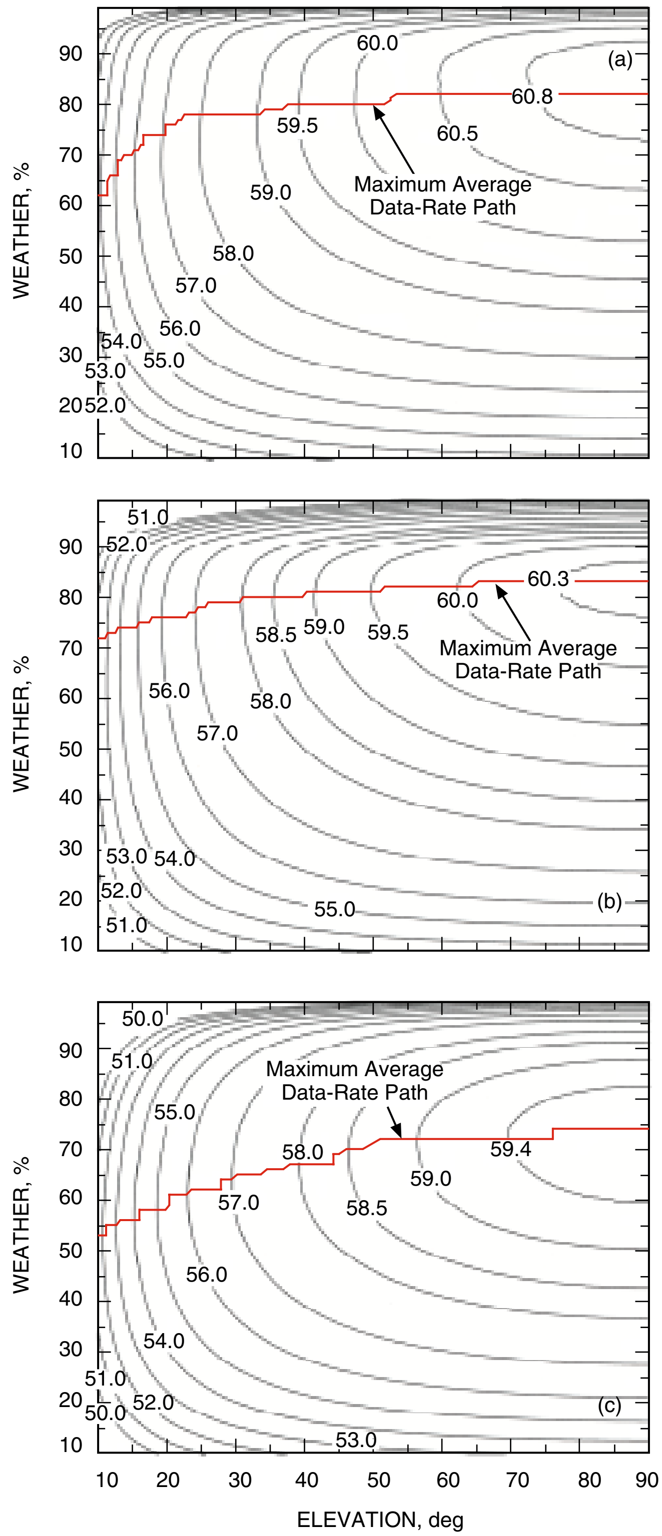

Fig. 4. Contours of average data rate versus elevation and weather percentile for W-band: (a) Goldstone, (b) Madrid, and (c) Canberra.

As these figures indicate, the higher the frequency, the lower is the weather reliability for the optimal performance of the link. Furthermore, as compared to the lower frequencies, the optimum weather reliability for higher frequencies is much lower at lower elevations than it is at higher elevations. This is because as the frequency increases so does the atmospheric noise. Since at lower elevations the signal travels through more atmosphere than it does at higher elevations, the cumulative effect of atmospheric noise is more pronounced at lower elevations. This means that for W-band and Ka-band, in order to make the link more reliable, the data rate needs to be substantially reduced, thus making the average performance of the link suboptimal.

Finally, note that the path of maximum ascent through each set of contours is approximated by a staircase type of function. This occurs because, at the points where the path of maximum ascent intersects the contours, the contours could be approximated by a vertical line. This means that at each elevation there is a range of weather percentile values that produces approximately the same average data rate as the optimum average data rate. This in turn makes it rather difficult to exactly calculate the optimum weather percentile value. Thus, this ambiguity leads to the stepwise nature of the approximation of the path of maximum ascent.

V. W-Band–Ka-Band–X-Band Link Comparison: The Thermometer Chart

Traditionally, the "thermometer chart" has been used to compare links at different frequencies. This chart plots the differences in each of the parameters in the link equation in order to provide a visual comparison. Figures 5 through 7 represent examples of these charts. These figures were obtained by assuming that the link operates at optimal weather percentile value at each site for each frequency and then comparing the performance of the link for different frequencies with each other, using Eq. (14) and the parameters shown in Table 3. Values in Table 3 are based on the information outlined in Section III. The values in this table are used throughout the analysis presented in this article unless it is noted otherwise.

Figures 5 through 7 were obtained for optimum weather at 30-deg elevation. Figure 5 shows the Ka-band advantage over X-band; Fig. 6 shows the W-band advantage over X-band; and Fig. 7 shows the W-band advantage (disadvantage) over Ka-band.

Table 3. Parameter values used in the analysis.

Parameter	X-band	Ka-band	W-band
Spacecraft amplifier efficiency, %	60	48	30
Spacecraft antenna size, m	2	2	2
Spacecraft antenna efficiency, %	85	85	85
Spacecraft antenna pointing loss, dB	0.0029	0.0423	0.3345
Ground antenna pointing loss, dB	0.0007	0.0099	0.0789
Ground antenna efficiency	810-5 X-band gain model for DSS-25 [1]	810-5 Ka-band gain model for DSS-25 [1]	18%
$T_{eq}(\theta)$	810-5 X-band model for dual-frequency non-diplexed 34-m BWG antenna with maser [1]	810-5 Ka-band model for dual-frequency non-diplexed 34-m BWG antenna [1]	50 K

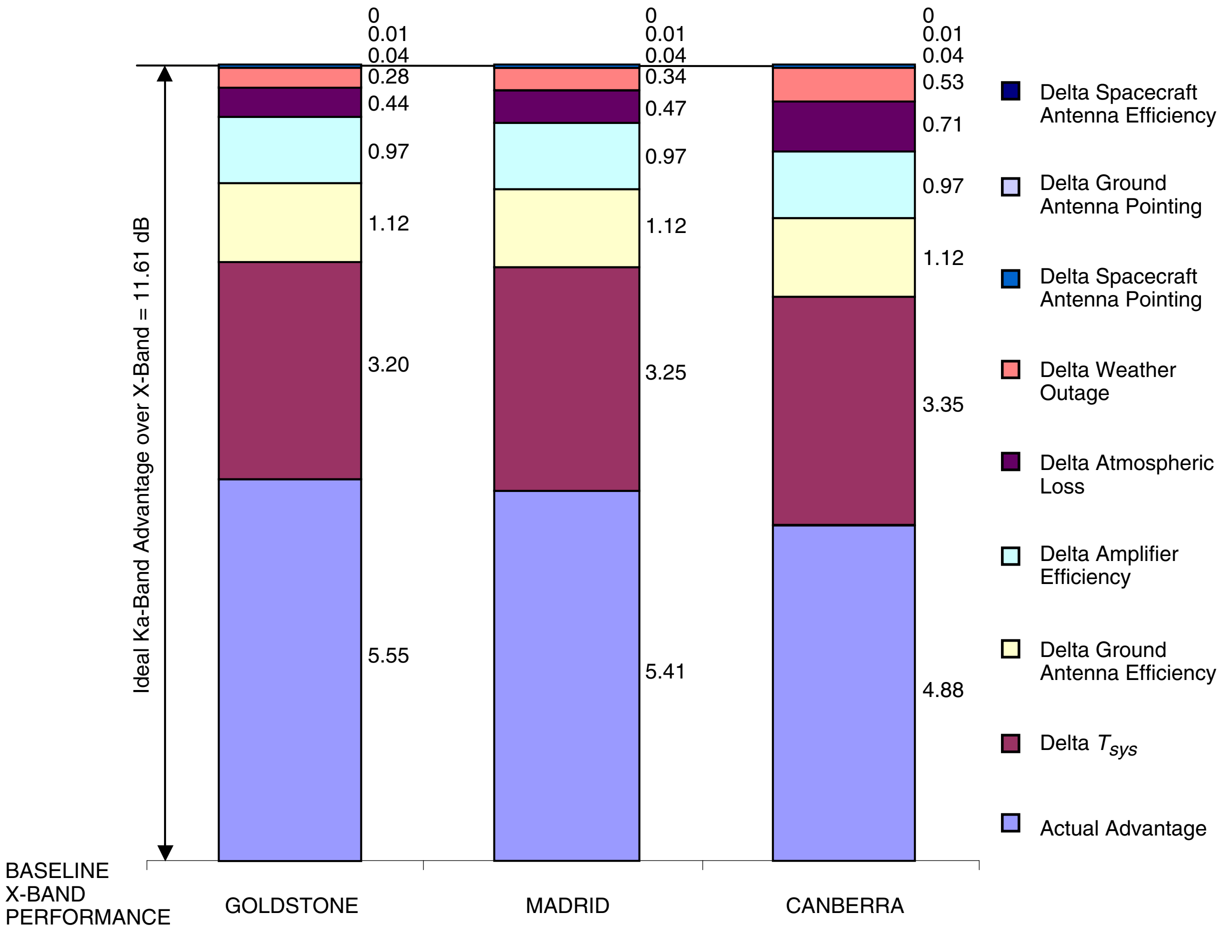

Fig. 5. Optimum Ka-band advantage over optimum X-band, 30-deg elevation.

As seen from these figures, the optimum Ka-band provides between 4.88 dB (Canberra) and 5.55 dB (Goldstone) more data at 30-deg elevation than the optimum X-band performance. W-band does not provide much better performance than X-band at 30-deg elevation and performs much worse than Ka-band given the configuration that was analyzed. Therefore, W-band does not seem like a good candidate for replacing Ka-band on the basis of average data return. It should also be noted that W-band has its worst performance at Canberra and its best performance at Goldstone, as Canberra is the wettest DSCC site and Goldstone is the driest.

VI. Break-Even (Compared to Ka-Band) W-Band Efficiency and W-Band–Ka-Band Performance Comparison

Looking at the thermometer charts in Fig. 7, it is obvious that the main reason that W-band is performing worse than Ka-band is poor ground antenna efficiency. The logical question then is how much the W-band antenna efficiency needs to be improved in order for W-band to perform at least as well as Ka-band. Using Eq. (11), this question is answered, and the results are plotted in Fig. 8. As seen from this figure, W-band efficiency needs to be significantly improved (to between 27 percent and 60 percent) from the current 18 percent in order for W-band to perform as well as Ka-band.

At lower elevations, the W-band antenna efficiency needs to be improved more than it does at higher elevations because the W-band atmospheric noise temperature is higher than that for Ka-band. Again,

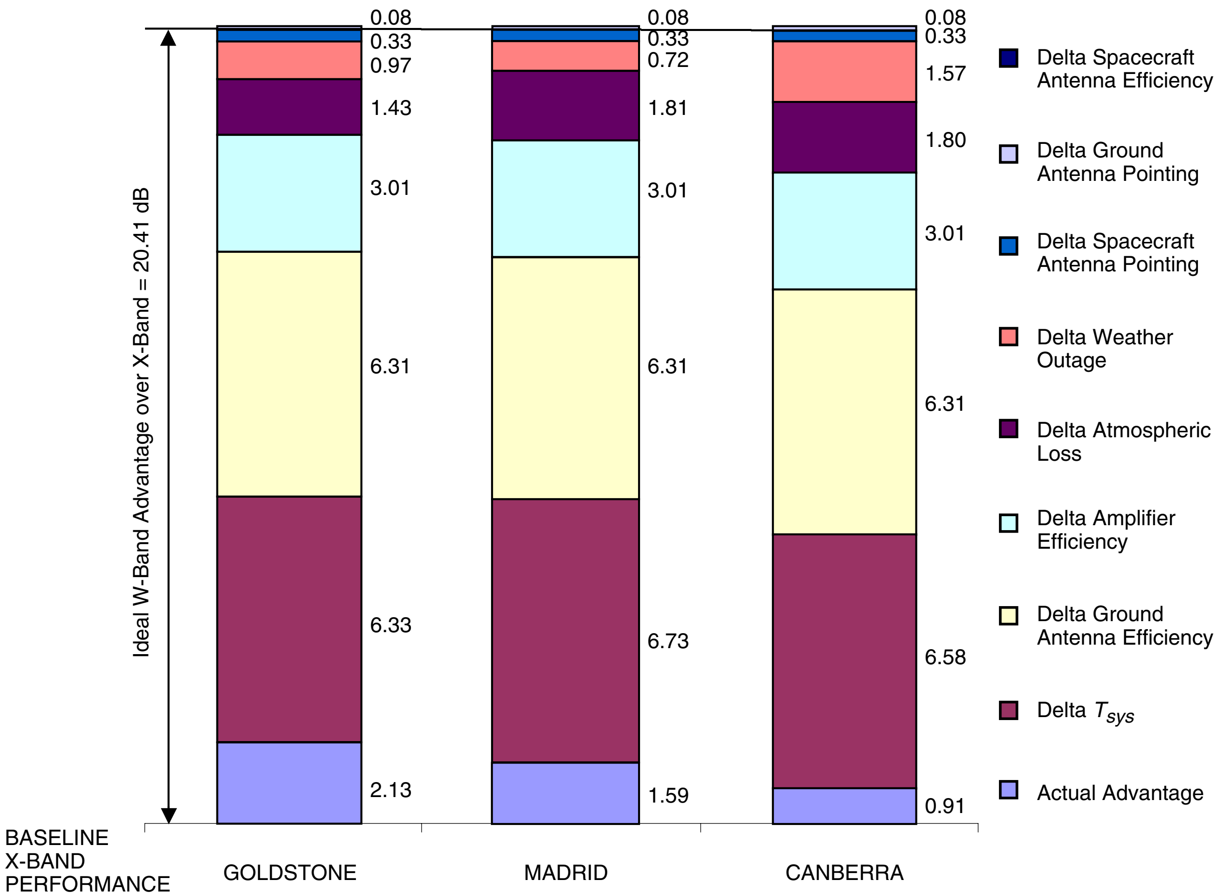

Fig. 6. Optimum W-band advantage over optimum X-band, 30-deg elevation.

as seen in Eq. (4), W-band's higher zenith atmospheric noise temperature translates to an even higher atmospheric noise temperature at lower elevations, thus increasing the difference between Ka-band and W-band atmospheric noise temperatures at lower elevations.

With 18 percent ground antenna efficiency, W-band performs substantially worse than does Ka-band. This is illustrated in Fig. 9. W-band performs between 2 and 5 dB worse than Ka-band depending on site and elevation. To improve the data return performance of W-band relative to Ka-band so that it becomes a viable alternative to Ka-band, the efficiency of the antenna at W-band needs to be substantially increased. Figure 10 illustrates the required antenna efficiency for different elevations at different sites so that the optimum W-band link will perform 2 dB better on the average than the optimum Ka-band link. As seen from this figure, for a W-band link to achieve this performance at 30-deg elevation, the antenna efficiency needs to be improved to better than 70 percent. This figure also indicates that only at elevations greater than 70 deg does the required efficiency of 2 dB better performance fall below 50 percent. It should be noted that improving the W-band antenna efficiency to 70 percent would also improve the Ka-band antenna efficiency, thus decreasing the W-band advantage to less than 2 dB.

Finally, two things should be noted. First, the analyses presented in the previous section and in this section were based on very optimistic assumptions about the performance of the W-band spacecraft amplifier. In all likelihood, the actual efficiency of a W-band amplifier will be much less than 30 percent. This will make the required break-even efficiency for W-band even greater than what has been calculated

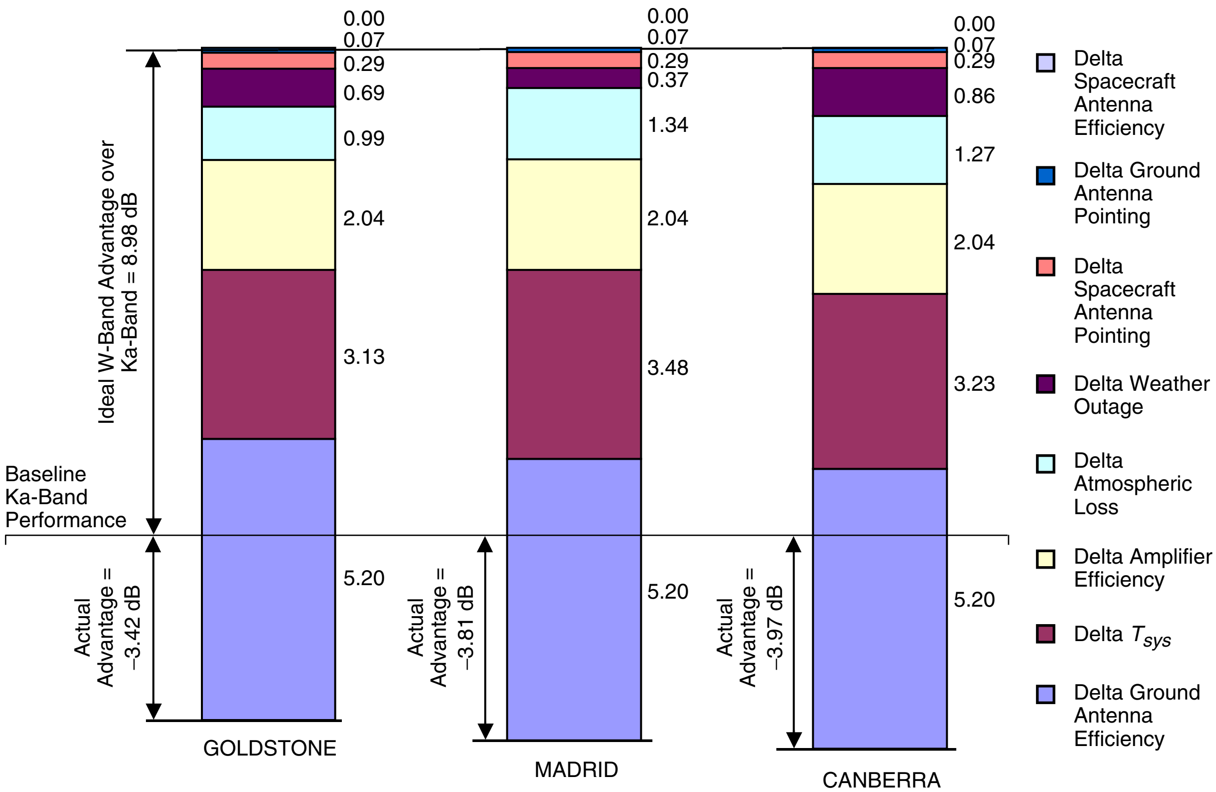

Fig. 7. Optimum W-band advantage over optimum Ka-band, 30-deg elevation.

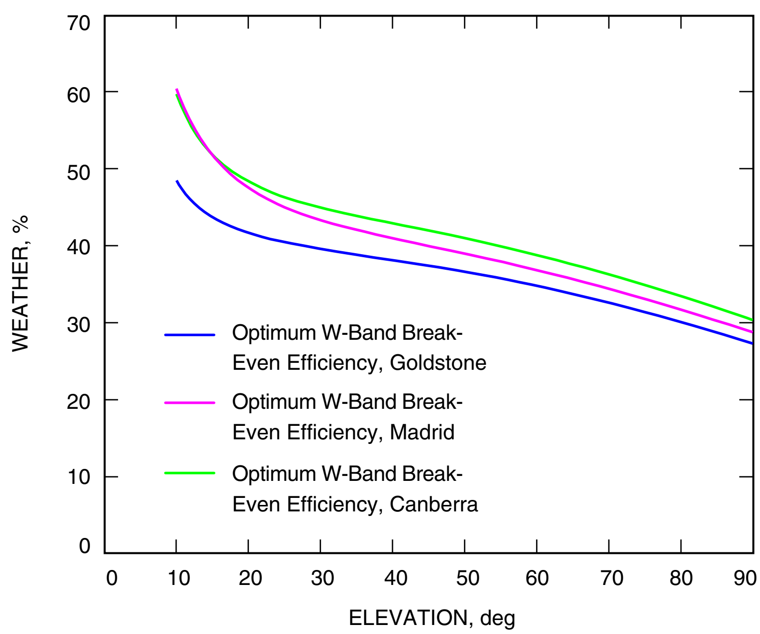

Fig. 8. W-band versus Ka-band break-even efficiency versus elevation.

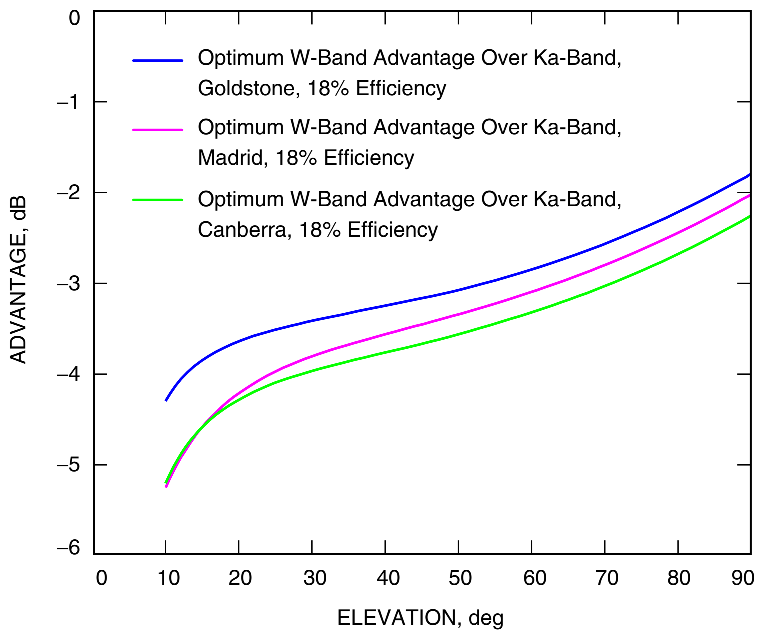

Fig. 9. W-band advantage over Ka-band versus elevation, 18 percent W-band ground antenna efficiency.

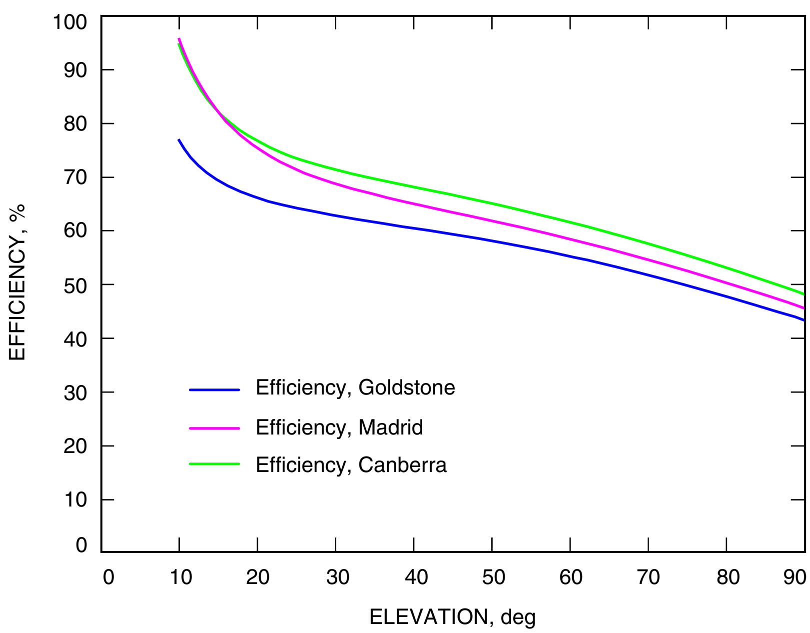

Fig. 10. Required W-band 34-m BWG antenna efficiency for 2-dB average data-rate advantage over Ka-band.

for this article. Secondly, the analysis presented here considers only the performance of W-band in terms of its data return capability. Other issues such as lack of bandwidth availability at Ka-band may force missions to consider W-band. W-band has greater usable bandwidth than either Ka-band or X-band, and this makes W-band attractive to high-data-rate missions without severe power constraints.

VII. Conclusions

In this article, a methodology for comparing the data-return capabilities of a projected W-band link with Ka-band and X-band links was developed. In this methodology, the performance of each band was measured in terms of optimum average data rate at a given elevation. Using formulas developed for calculating W-band atmospheric noise temperature from 31.4-GHz atmospheric noise-temperature measurements by water-vapor radiometers, cumulative distribution functions for W-band zenith atmospheric noise temperature were calculated for the three Deep Space Communication Complexes. Using these distributions along with information about the performance of current and potential W-band components and actual performance of Ka-band and X-band equipment, the optimum performances of X-band, Ka-band, and W-band were calculated. In addition, thermometer charts for performance comparison of W-band with X-band, W-band with Ka-band, and Ka-band with X-band were obtained for 30-deg elevation for all three DSCCs for a 34-m BWG antenna. Based on these thermometer charts, the W-band performance is only marginally better than X-band and significantly (∼3.5-dB) worse than Ka-band at 30-deg elevation for all three sites. In addition, the W-band–Ka-band break-even efficiencies for different elevations were calculated for all three sites. This exercise showed that the W-band 34-m BWG antenna efficiency needs to be improved significantly over its current 18 percent (to between 27 percent and 60 percent depending on location and elevation) in order for W-band to have the same performance as Ka-band. Furthermore, the performance of W-band was compared to Ka-band over a range of elevations. This comparison showed that with 18 percent efficiency W-band performs significantly (between 2 and 5 dB) worse than Ka-band over the whole range of elevations. Finally, for a range of elevations, the W-band antenna efficiencies that offered a W-band performance that is 2 dB better than the Ka-band performance were calculated. These calculations indicate that, below 70-deg elevation, the W-band antenna efficiency needs to be much better than 50 percent (>70 percent at 30-deg elevation) in order for W-band to have a 2-dB performance advantage over Ka-band. Based on these results and noting that the values of some parameters used in this exercise (specifically, the spacecraft amplifier efficiency) have been overly optimistic, it is the conclusion of this article that W-band is not recommended for use by missions with tight power constraints. However, since W-band offers more bandwidth than either X-band or Ka-band, missions with high data rates may be forced to use it.

Acknowledgments

The author would like to thank Stephen Keihm for providing him with formulas for converting Ka-band atmospheric noise temperature measurements to W-band values. The author would also like to thank Dr. Christian Ho for reviewing this article.

References

[1] S. D. Slobin, "34-m BWG Stations Telecommunications Interfaces," *DSMS Telecommunications Link Design Handbook,* 810-005, Rev. E, Module 104, Jet Propulsion Laboratory, Pasadena, California, November 30, 2000.

[2] S. D. Slobin, "Atmospheric and Environmental Effects," *DSMS Telecommunications Link Design Handbook,* 810-005, Rev. E, Module 105, Rev. A, Jet Propulsion Laboratory, Pasadena, California, December 15, 2002.